nature geoscience

LETTERS

PUBLISHED ONLINE: 16 SEPTEMBER 2012 | DOI: 10.1038/NGEO1568

Sensitivity of tropical precipitation extremes to climate change

Paul A. O'Gorman

Precipitation extremes increase in intensity over many regions of the globe in simulations of a warming climate[1–3]. The rate of increase of precipitation extremes in the extratropics is consistent across global climate models, but the rate of increase in the tropics varies widely, depending on the model used[3]. The behaviour of tropical precipitation can, however, be constrained by observations of interannual variability in the current climate[4–6]. Here I show that, across state-of-the-art climate models, the response of tropical precipitation extremes to interannual climate variability is strongly correlated with their response to longer-term climate change, although these responses are different. I then use satellite observations to estimate the response of tropical precipitation extremes to the interannual variability. Applying this observational constraint to the climate simulations and exploiting the relationship between the simulated responses to interannual variability and climate change, I estimate a sensitivity of the 99.9th percentile of daily tropical precipitation to climate change at 10% per K of surface warming, with a 90% confidence interval of 6–14% K^{-1}. This tropical sensitivity is higher than expectations for the extratropics[3] of about 5% K^{-1}. The inferred percentage increase in tropical precipitation extremes is similar when considering only land regions, where the impacts of extreme precipitation can be severe.

Increases in precipitation extremes (defined here as high percentiles of daily precipitation) associated with climate change would have important impacts, such as on flooding, soil erosion, and landslides[7,8]. Changes in the distribution of precipitation are expected in a warmer climate because of the dependence of the saturation vapour pressure of water on temperature[3,9,10]. Observations suggest that precipitation extremes may have increased in intensity as the climate warmed in recent decades, at least regionally[11,12]. Extratropical precipitation extremes consistently increase at close to the 'thermodynamic' rate ($\sim$6% K^{-1}) in simulations with global climate models, corresponding to little change in the magnitude of vertical winds associated with the extremes[3]. The thermodynamic rate is similar in the tropics, but the simulated rate of increase of tropical precipitation extremes may be substantially lower or higher depending on the model used, with close to no change in some models and rates of increase of up to 30% K^{-1} in others[3]. This inter-model scatter probably results from the strong dependence of tropical precipitation on moist-convective processes that must be represented by subgrid parameterizations in global climate-change simulations[13]. Recent idealized studies of radiative-convective equilibrium using models that resolve convective-scale dynamics found that intense precipitation increases with warming at close to the thermodynamic rate[14,15], but a different response could occur in the tropics because of convective organization and large-scale dynamics that were not included in the idealized studies.

Given that climate models simulate robust large-scale patterns of temperature change in the tropics[16] but have difficulty in reliably simulating tropical precipitation extremes, it is reasonable to ask whether observations of temperature and precipitation may be used to help constrain the expected response of tropical precipitation extremes to climate change. Studies of observed variability within the current climate suggest stronger increases in certain types of precipitation extremes with warming than given by the thermodynamic rate[4,5,17]. But the sensitivity of precipitation extremes to temperature changes within a given climate cannot be assumed to be the same as the sensitivity under climate change. For example, interannual variability in tropical precipitation extremes is largely related to El Niño-Southern Oscillation (ENSO), which has distinct temperature patterns and dynamics compared with global warming[18,19].

Here, I show that the sensitivity of tropical precipitation extremes to temperature changes associated with variability is in fact strongly correlated across models with the sensitivity for global warming (although the sensitivities are not the same). I use this relationship between sensitivities for variability and climate change, together with observations of variability, to constrain the climate-change sensitivity of tropical precipitation extremes. Similar approaches have previously been used to constrain snow-albedo feedback[20] and climate sensitivity[21] using the observed seasonal cycle. An important feature of the approach presented here is that it is physically plausible that the same subgrid parameterizations responsible for moist convection (and the division between convective and stratiform rainfall) cause the inter-model scatter in the response of tropical precipitation extremes to both variability and climate change.

The default simulations used involve 18 climate models from the World Climate Research Programme's Coupled Model Intercomparison Project phase 3 (CMIP3) archive. Simulated variability is analysed over the period 1981–2000 in the 20C3M simulation, and climate change is calculated as the difference between this period and 2081–2100 in the SRES-A1B scenario (slightly different time periods are used for some models; see Supplementary Information). The analysis was also repeated for a subset of 'good-ENSO' climate models that have been identified as having ENSO temperature variability similar to that found in observations[22], and for simulations drawn from the recently available CMIP5 archive. The default precipitation observations are taken from the Special Sensor Microwave Imager (SSM/I) using the dataset from Remote Sensing Systems (RSS) over the period 1991–2008 (ref. 23), and four other observational precipitation datasets are used for comparison. Surface temperatures are taken from the National Oceanic and Atmospheric Administration Merged Land–Ocean Surface Temperature Analysis[24]. Climate change is calculated over the whole tropics or over tropical land, whereas variability is

Massachusetts Institute of Technology, Cambridge, Massachusetts 02139, USA. *e-mail: pog@mit.edu.

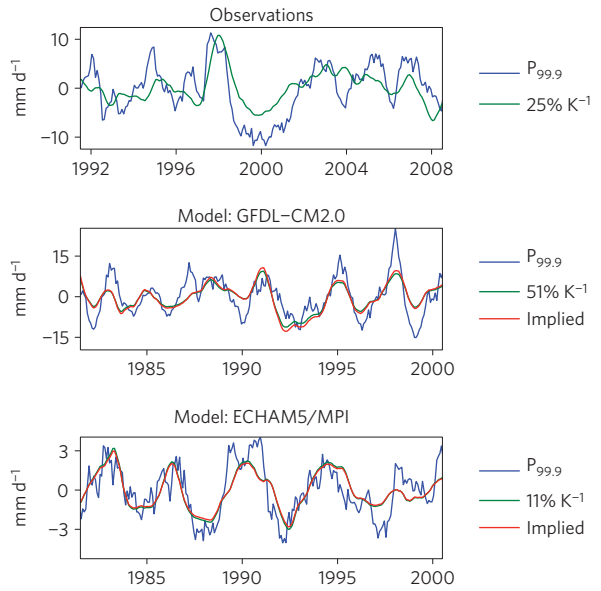

Figure 1 | Time series of precipitation extremes and surface temperature over the tropical oceans in observations and simulations (GFDL-CM2.0 and ECHAM5/MPI). Anomalies in the 99.9th percentile of precipitation (blue) and surface temperature rescaled by the sensitivity (% K^{-1}) for variability in each case (green) are shown. Also shown (red) for the models are surface temperature anomalies rescaled by the sensitivity for variability implied by the sensitivity for climate change (over the whole tropics) and the regression relationship between sensitivities for variability and climate change for all the CMIP3 models (Supplementary Table S1). Time series are filtered with a 6-month running average.

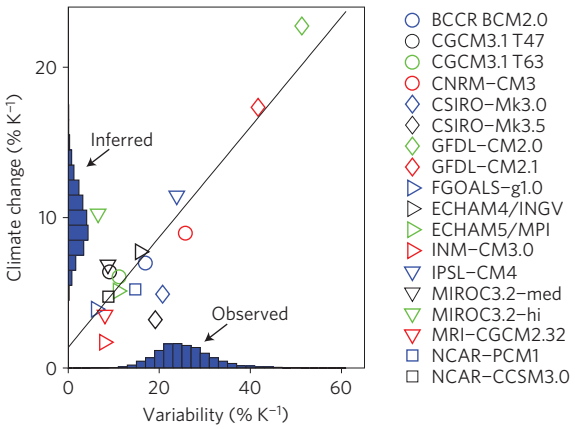

Figure 2 | Sensitivities (% K^{-1}) of the 99.9th percentile of precipitation for variability versus climate change in the CMIP3 simulations. The solid line shows the ordinary-least-squares best fit. Histograms show estimates (with uncertainty) of the observed sensitivity for variability and the inferred sensitivity for climate change. Sensitivities for variability are over the tropical oceans and sensitivities for climate change are over the whole tropics.

generally analysed over the tropical oceans because this is found to give the strongest constraint on sensitivities for climate change. Results are also reported using variability over the whole tropics.

Time series are first constructed of precipitation extremes and mean surface temperature over the tropical oceans between 30° S and 30° N (Methods). The influence of ENSO on precipitation extremes over the tropical oceans is clearly evident in observations, as shown in Fig. 1 for the 99.9th percentile of daily precipitation and consistent with results from previous studies[4–6]. Positive anomalies in surface temperature tend to be associated with positive anomalies in precipitation extremes; the calculated sensitivity to surface temperature (Methods) is 25% K^{-1} with a 90% confidence interval of 16–36% K^{-1}. A similar behaviour is found in the climate-model simulations, but with different time series of surface temperature because coupled models are considered, and with very different sensitivities depending on the climate model used (Fig. 1 and Supplementary Fig. S1).

Sensitivities for climate change are calculated over the whole tropics in the climate model simulations and are normalized by changes in mean surface temperature (Methods). For the 99.9th percentile of precipitation, the sensitivities for climate change are strongly correlated across models with the sensitivities for variability (Fig. 2), with a correlation coefficient of 0.866. The relationship between sensitivities is further quantified using ordinary-least-squares regression (Supplementary Table S1). The regression line passes close to the origin, and the sensitivity for variability is greater than the sensitivity for climate change by roughly a factor of 2.5.

The relationship between the sensitivities for variability and climate change, together with the observed sensitivity for variability, yields an inferred sensitivity for climate change. For the 99.9th percentile of precipitation, the inferred sensitivity for climate change is 10% K^{-1}, which is higher than what most of the models simulate (Fig. 2). Uncertainty is estimated by a bootstrapping procedure involving resampling of the models used and 12-month blocks in the observed and simulated time series (Methods). The resulting 90% confidence interval of 6–14% K^{-1} is substantially narrower than the inter-model scatter of 2–23% K^{-1}, clearly illustrating the value of the observational constraint.

The inferred sensitivity for climate change increases with percentile from the 98th to the 99.9th percentile and decreases slightly to the 99.95th percentile (Fig. 3a); it generally exceeds the multimodel-median sensitivity (and by as much as 68%), although it maximizes at the 99.9th percentile whereas the multimodel median continues to increase with percentile. Both intermodel scatter and the strength of the relationship between sensitivities for variability and climate change increase with percentile (Supplementary Table S1), such that the observational constraint is more useful for higher percentiles of precipitation.

The inferred sensitivities were also calculated for climate change over land only, with variability over the ocean as before. A strong relationship holds between climate change and variability for the higher percentiles of precipitation considered (Supplementary Fig. S2 and Table S2), and the inferred sensitivities for climate change over land approach the sensitivities over the whole tropics at these percentiles (Fig. 3b). This similar response over land and the whole tropics occurs despite ~60% greater surface warming over land than ocean (all sensitivities for climate change are normalized by temperature changes over the whole tropics for ease of comparison). Indeed, the percentage changes in precipitation extremes in the simulations of climate change are close to equal over land and ocean across all the models (Supplementary Fig. S3), which is likely related to the importance of oceanic water vapour sources for precipitation over land and to decreases in land surface-air relative humidity under global warming[25].

For the 'good-ENSO' subset of models (Supplementary Information), the relationship between sensitivities for climate change and variability is very tight for the 99.9th percentile of precipitation (Supplementary Fig. S4), with a correlation coefficient of 0.997, and the resulting inferred sensitivities for climate change are similar to what is obtained using all the models (Supplementary Table S1). This robustness suggests that the inferred response to climate change is not strongly affected by the relatively poor quality of simulated ENSO temperature variability in some of the model simulations. Similar results are also obtained using the CMIP5

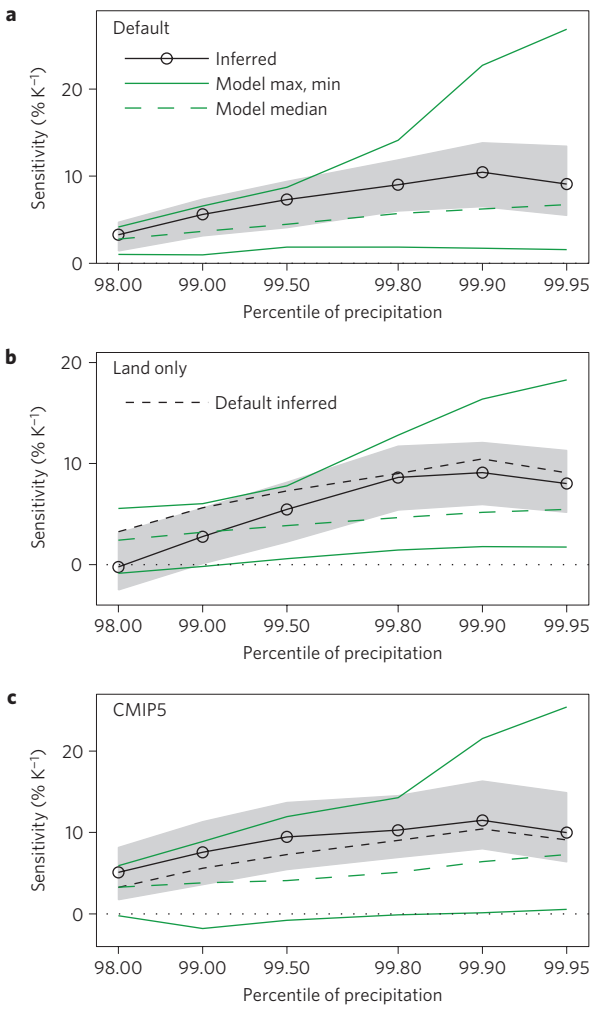

Figure 3 | Inferred and simulated climate-change sensitivities (% K^{-1}) for high percentiles of precipitation. Black lines with circles show inferred sensitivities, shading shows the associated 90% confidence intervals, solid green lines show multimodel maxima and minima, and dashed green lines shows multimodel medians. **a**, CMIP3 models and the whole tropics. **b** as in **a** but for climate change over land only and normalized by temperature changes over the whole tropics. **c** as in **a** but for CMIP5 models. Black dashed lines in **b**,**c** reproduce the inferred sensitivities shown in **a**.

simulations; the relationship between sensitivities for variability and climate change is less tight than in CMIP3 for the 99.9th percentile of precipitation (Supplementary Fig. S5 and Table S3), but the inferred sensitivities for climate change are only slightly higher, at 11% K^{-1} versus 10% K^{-1} (Fig. 3c).

To help assess uncertainties related to observational estimation of precipitation (which are not included in the estimates of uncertainty given above), the analysis was repeated for four alternative observational precipitation datasets: the Goddard Profiling Algorithm (GPROF; ref. 26) applied to SSM/I radiances, a dataset from the Tropical Rainfall Measuring Mission (TRMM) Microwave Imager (TMI), the 1-degree daily merged dataset from the Global Precipitation Climatology Project (GPCP 1DD; ref. 27), and the TRMM 3B42 merged daily dataset[28]. Most of these alternative precipitation datasets cover a shorter time period than the default precipitation dataset, but they all give similar inferred sensitivities for climate change (Supplementary Table S4 and Fig. S6). Similar results are also obtained whether variability is calculated over the whole tropics or over the tropical oceans (using the SSM/I GPROF dataset because the default precipitation dataset does not include values over land), despite different relationships between variability and climate change in each case (Supplementary Table S5).

The results presented show how the simulated response to climate change of an important aspect of the tropical hydrological cycle may be constrained using observed variability. The inferred sensitivities of tropical precipitation extremes under climate change have ranges of uncertainty that are considerably narrower than the intermodel scatter. The inferred sensitivity of 10% K^{-1} (with a 90% confidence interval of 6–14% K^{-1}) for the 99.9th percentile of tropical precipitation is higher than what climate models simulate for the same percentile of extratropical precipitation (3–6% K^{-1} across models and 5% K^{-1} in the multimodel median[3]). A higher sensitivity in the tropics than the extratropics is physically possible if, for example, the circulations associated with precipitation extremes strengthen with warming in the tropics whereas they remain roughly constant in the extratropics[3]. One caveat is that other sensitivities may apply at hourly timescales for extratropical convective storms[17]. The similarity of the inferred response when the analysis is restricted to climate change over tropical land regions only (for sufficiently high percentiles of precipitation) is important for impacts of climate change, and it suggests that precipitation extremes over land may be more strongly tied to changes in surface temperatures over ocean rather than land. The observational constraint provides additional motivation for monitoring of tropical precipitation and efforts to better understand the associated observational uncertainties. Consistent estimates were obtained from only a decade of observations for three of the datasets considered (Supplementary Table S4), which suggests that the analysis could be applied reasonably quickly to data from new observing platforms. Ongoing research continues to lead to improvements in the parameterization of moist convection in climate models, but precipitation extremes are particularly challenging for convective parameterizations[13] and observational constraints are expected to continue to be useful.

Methods

Calculation of sensitivities. Details of the climate models and observational datasets used are given in the Supplementary Information. All precipitation datasets are first conservatively interpolated to an equal-area grid with constant spacing in longitude of 3°. The interpolation method is first order and weights data according to the area of overlap between gridboxes in the original and coarse grid[29], consistent with the treatment of precipitation as a flux[30]. The use of a conservative interpolation scheme and a relatively-coarse common grid helps to allow for a fair comparison of precipitation extremes in observations and simulations with different native resolutions[30] and improves the robustness of the observational estimates. For the SSM/I and TMI observational datasets, both ascending and descending passes are given equal weight in the interpolation when available.

Time series of surface temperature and precipitation extremes are constructed as follows. For each month, daily precipitation rates are aggregated in time over the month and in space between 30° S and 30° N. Precipitation extremes are then calculated as high percentiles of the aggregated precipitation rates (including rates equal to zero) to yield one value per month for each percentile. Given a balance between the desire to study extreme precipitation and a sample size of roughly 70,000 precipitation rates per month or less, the 99.9th percentile is the primary focus, but results for other percentiles are also reported. Monthly surface temperature is spatially averaged between 30° S and 30° N (again giving one value per month). Surface skin temperatures are consistently used throughout the paper, with the exception of the results in Supplementary Table S5, for which the observed temperatures over land are surface air temperatures.

In the case of sensitivities for variability, the time series of precipitation extremes and surface temperature are calculated either over the whole tropics or over the tropical oceans (30° S to 30° N). The time series are deseasonalized by subtracting the mean seasonal cycle as estimated from the time series themselves. The time series are then detrended and filtered with a 6-month running average, followed by ordinary-least-squares regression of precipitation extremes against surface temperature. The calculated sensitivities (% K^{-1}) are expressed as a fraction of the mean value of the precipitation extremes over the time period. This simple sensitivity for variability is adequate, despite the spatially heterogeneous response to ENSO, because it is used as an observable that is strongly correlated with the sensitivity for climate change and not to fully characterize the response of precipitation to ENSO.

In the case of sensitivities for climate change, the time series for precipitation and surface temperature described above are calculated either over the whole tropics or over tropical land (30° S to 30° N). The time series are then averaged over the twentieth and twenty-first century time periods, and the climate-change sensitivity of precipitation extremes (% K^{-1}) is expressed as the difference in precipitation extremes normalized by their twentieth century value and the difference in surface temperature.

Relatively strict land and ocean masks are used in this study. The masks are specified such that grid boxes with less than 90% ocean are excluded when considering ocean, and grid boxes with less than 90% land are excluded when considering land. The masks are applied after interpolation to the common grid in the case of precipitation. The use of a relatively strict mask is needed for consistency between the observational datasets for ocean-only precipitation; the SSM/I RSS dataset has missing values over land that would bias the sensitivities for variability otherwise. The use of a relatively strict mask also helps to minimize the contribution of ocean precipitation when calculating climate change over land in the climate-model simulations.

Estimation of uncertainty. Uncertainty is estimated using a bootstrapping method. A total of 2,000 bootstrap estimates of the inferred sensitivity for climate change are generated by resampling both the models used and the time series for models and observations. Time series are resampled using 12-month moving blocks because of autocorrelation in the time series; use of shorter blocks results in smaller error estimates. In the case of the model time series, resampled time series are used in the calculation of the sensitivities for both variability and climate change. The same block resampling of time series is used in the calculation of confidence intervals of the sensitivities for variability.

It is important to note that the estimates of uncertainty do not account for errors in the estimation of observed precipitation rates (see Supplementary Fig. S6 and Table S4). Note also that the models used are not truly independent. For example, models GFDL-CM2.0 and GFDL-CM2.1 are developed at the same laboratory and share many of the same components. At a minimum, the simulations from these models may be regarded as giving independent realizations with a similar physical model.

Received 14 February 2012; accepted 6 August 2012; published online 16 September 2012

References

1. Kharin, V. V., Zwiers, F. W., Zhang, X. & Hegerl, G. C. Changes in temperature and precipitation extremes in the IPCC ensemble of global coupled model simulations. *J. Clim.* **20,** 1419–1444 (2007).
2. Sun, Y., Solomon, S., Dai, A. & Portmann, R. W. How often will it rain? *J. Clim.* **20,** 4801–4818 (2007).
3. O'Gorman, P. A. & Schneider, T. The physical basis for increases in precipitation extremes in simulations of 21st-century climate change. *Proc. Natl Acad. Sci. USA* **106,** 14773–14777 (2009).
4. Allan, R. P. & Soden, B. J. Atmospheric warming and the amplification of precipitation extremes. *Science* **321,** 1481–1484 (2008).
5. Allan, R. P., Soden, B. J., John, V. O., Ingram, W. & Good, P. Current changes in tropical precipitation. *Environ. Res. Lett.* **5,** 025205 (2010).
6. Liu, C. & Allan, R. P. Multisatellite observed responses of precipitation and its extremes to interannual climate variability. *J. Geophys. Res.* **117,** D03101 (2012).
7. Parry, M. L. *et al.* in *IPCC Climate Change 2007: Impacts, Adaptation and Vulnerability* (eds Parry, M. L. *et al.*) 23–78 (Cambridge Univ. Press, 2007).
8. Pall, P. *et al.* Anthropogenic greenhouse gas contribution to flood risk in England and Wales in autumn 2000. *Nature* **470,** 382–385 (2011).
9. Trenberth, K. E., Dai, A., Rasmussen, R. M. & Parsons, D. B. The changing character of precipitation. *Bull. Am. Meteorol. Soc.* **84,** 1205–1217 (2003).
10. O'Gorman, P. A. & Schneider, T. Scaling of precipitation extremes over a wide range of climates simulated with an idealized GCM. *J. Clim.* **22,** 5676–5685 (2009).
11. Groisman, P. Y. *et al.* Trends in intense precipitation in the climate record. *J. Clim.* **18,** 1326–1350 (2005).
12. Min, S. K., Zhang, X., Zwiers, F. W. & Hegerl, G. C. Human contribution to more-intense precipitation extremes. *Nature* **470,** 378–381 (2011).
13. Wilcox, E. M. & Donner, L. J. The frequency of extreme rain events in satellite rain-rate estimates and an atmospheric general circulation model. *J. Clim.* **20,** 53–69 (2007).
14. Muller, C. J., O'Gorman, P. A. & Back, L. E. Intensification of precipitation extremes with warming in a cloud resolving model. *J. Clim.* **24,** 2784–2800 (2011).
15. Romps, D. M. Response of tropical precipitation to global warming. *J. Atmos. Sci.* **68,** 123–138 (2011).
16. Sobel, A. H. & Camargo, S. J. Projected future seasonal changes in tropical summer climate. *J. Clim.* **24,** 473–487 (2011).
17. Lenderink, G. & Van Meijgaard, E. Increase in hourly precipitation extremes beyond expectations from temperature changes. *Nature Geosci.* **1,** 511–514 (2008).
18. Lu, J., Chen, G. & Frierson, D. M. W. Response of the zonal mean atmospheric circulation to El Niño versus global warming. *J. Clim.* **21,** 5835–5851 (2008).
19. Chou, C. & Tu, J. Y. Hemispherical asymmetry of tropical precipitation in ECHAM5/MPI-OM during El Niño and under global warming. *J. Clim.* **21,** 1309–1332 (2008).
20. Hall, A. & Qu, X. Using the current seasonal cycle to constrain snow albedo feedback in future climate change. *Geophys. Res. Lett.* **33,** L03502 (2006).
21. Knutti, R., Meehl, G. A., Allen, M. R. & Stainforth, D. A. Constraining climate sensitivity from the seasonal cycle in surface temperature. *J. Clim.* **19,** 4224–4233 (2006).
22. Guilyardi, E. *et al.* Understanding El Niño in ocean–atmosphere general circulation models. *Bull. Am. Meteorol. Soc.* **90,** 325–340 (2009).
23. Hilburn, K. A. & Wentz, F. J. Intercalibrated passive microwave rain products from the unified microwave ocean retrieval algorithm (UMORA). *J. Appl. Meteorol.* **47,** 778–794 (2008).
24. Smith, T. M., Reynolds, R. W., Peterson, T. C. & Lawrimore, J. Improvements to NOAA's historical merged land–ocean surface temperature analysis (1880–2006). *J. Clim.* **21,** 2283–2296 (2008).
25. O'Gorman, P. A. & Muller, C. J. How closely do changes in surface and column water vapor follow Clausius–Clapeyron scaling in climate-change simulations? *Environ. Res. Lett.* **5,** 025207 (2010).
26. Kummerow, C. *et al.* The evolution of the Goddard Profiling Algorithm (GPROF) for rainfall estimation from passive microwave sensors. *J. Appl. Meteorol.* **40,** 1801–1820 (2001).
27. Huffman, G. J. *et al.* Global precipitation at one-degree daily resolution from multisatellite observations. *J. Hydrometeorol.* **2,** 36–50 (2001).
28. Huffman, G. J. *et al.* The TRMM multisatellite precipitation analysis (TMPA): Quasi-global, multiyear, combined-sensor precipitation estimates at fine scales. *J. Hydrometeorol.* **8,** 38–55 (2007).
29. Jones, P. W. First- and second-order conservative remapping schemes for grids in spherical coordinates. *Mon. Weath. Rev.* **127,** 2204–2210 (1999).
30. Chen, C. T. & Knutson, T. On the verification and comparison of extreme rainfall indices from climate models. *J. Clim.* **21,** 1605–1621 (2008).

Acknowledgements

I am grateful to C. Kummerow, T. Schneider, M. Tingley, R. Allan, K. Emanuel, C. Wunsch, S. Solomon and T. Merlis for helpful discussions. I acknowledge the World Climate Research Programme's Working Group on Coupled Modelling, which is responsible for CMIP, and I thank the climate modelling groups for producing and making available their model output. For CMIP the US Department of Energy's Program for Climate Model Diagnosis and Intercomparison provides coordinating support and led development of software infrastructure in partnership with the Global Organization for Earth System Science Portals. SSM/I (V6) data were provided by RSS (www.remss.com) and sponsored by the NASA Earth Science MEaSUREs DISCOVER Project. SSM/I and TMI GPROF (V10) data were downloaded from http://rain.atmos.colostate.edu/. GPCP 1DD (V1.1) data were downloaded from http://www1.ncdc.noaa.gov/pub/data/gpcp/. TRMM 3B42 (V7) daily data were provided by the Goddard Earth Sciences Data and Information Services Center. NOAA Merged Air Land and SST anomalies (V3.5.1) were provided by the NOAA/OAR/ESRL PSD from their website at http://www.esrl.noaa.gov/psd/. I acknowledge support from NSF grant AGS-1148594 and NASA grant NNX-11AO92G.

Additional information

Supplementary information is available in the online version of the paper. Reprints and permissions information is available online at www.nature.com/reprints.

Competing financial interests

The author declares no competing financial interests.